International Journal of Pharmaceutical Research and Applications
Volume 7, Issue 1 Jan-Feb 2022, pp: 961-987 www.ijprajournal.com ISSN: 2249-7781

Formulation, Optimization, and Evaluation of Nanostructured lipid Carriers of Resveratrol

Kannekanti Teja, Asha Spandana K M*, Dr Amit B Patil, Preethi S
Department of Pharmaceutics, JSS College of Pharmacy, Mysuru

Submitted: 05-02-2022 Accepted: 18-02-2022

ABSTRACT

Aim: The aim of this study was to optimize the formulation of Resveratrol-loaded Nanolipid carriers intended for brain targeting.

Purpose: To potentiate the neuroprotective effect of Resveratrol by improving its blood-brain barrier penetration through formulating the drug into nanostructured lipid carriers (NLCs)

Methods: A 2×3 factorial design was used to obtain 17 Resveratrol-NLCs; by using three factors on different levels the responses of prepared formulation were evaluated. Coconut oil, Tween 80, stearic acid, ethanol was chosen as liquid lipid, surfactant, solid lipid, and cosurfactant, respectively. RES-NLCs were prepared by the high shear hot homogenization technique followed by the ultrasonication method. Optimization was done based on the evaluation results using the box Behnken design.

Result: The optimized formulation had a particle size (PS) of 126 nm and zeta potential of (ZP) of -27.6 mv. The poly dispersibility index (PDI) and entrapment efficiency (EE) were found to be 0.327 and 70.18 ± 4.5% respectively. furtherly the formulations are subjected to stability studies by following ICH guidelines and the optimized formulations are stable in 25ºC/60% RH up to 3 months and morphological studies of the formulation were screened by using a scanning electron microscope the results of SEM showed that Resveratrol-NLC was spherical in shape. Finally, the optimized and stable formulation was tested for the in-vitro release pattern by mimicking the ivivo brain physiological conditions; the in-vitro drug release study has exhibited a sustained release of drug from the NLC. The kinetics of the release rate of Resveratrol NLC follows zero-order kinetics and is released by the diffusion process.

Keywords: Resveratrol; Nano lipid carrier systems; Homogenization; in-vitro drug release; the blood-brain barrier.

I. INTRODUCTION

[1,2]. Resveratrol was first extracted in the year 1940 from the roots of white hellebore (Veratrum grandiflorum) later Resveratrol (trans-resveratrol) has been one of the well-known polyphenols extracted from polygonaceous plants of grapes, and many more other species like red grapes, mulberries, and blueberries and in other trees, such as eucalyptus, spruce, and lily, as well as in other products such as peanuts. The most abundant natural sources of Resveratrol are Vitis vinifera, labrusca, and muscadine grapes, Polygonum cuspidatumSieb, previously a wide range of theoretical and applied studies have been carried out on the potential advantages of resveratrol, such as anti-inflammatory action, anti-carcinogenic action, anti-oxidant properties, anti-aging function, neuroprotective action. [3]. Resveratrol has drawn a great deal of attention in the food, pharmaceutical, and cosmetic industries due to its benefit to human health. However, trans-resveratrol is very unstable, particularly when exposed to light, if trans form of resveratrol converts to cis-resveratrol its bioactivity will decrease. Resveratrol has numerous mechanisms of action that interact with a wide range of molecular targets, but its beneficial effect on human health appears primarily to be related to its antioxidant activity. Since oxidative stress tends to be strongly linked to major neurological pathologies, Resveratrol has been evaluated for successful outcomes in neurodegenerative disorders including Alzheimer's disease (AD), Parkinson's disease, cerebral ischemia,(PD)Huntington's disease (HD), prion, epilepsy, and amyotrophic lateral sclerosis (ALS) however there are a variety of studies explaining the dose dependence of the drug on these health benefits. The mechanism action of Resveratrol is shown in Figure1.

International Journal of Pharmaceutical Research and Applications
Volume 7, Issue 1 Jan-Feb 2022, pp: 961-987 www.ijprajournal.com ISSN: 2249-7781

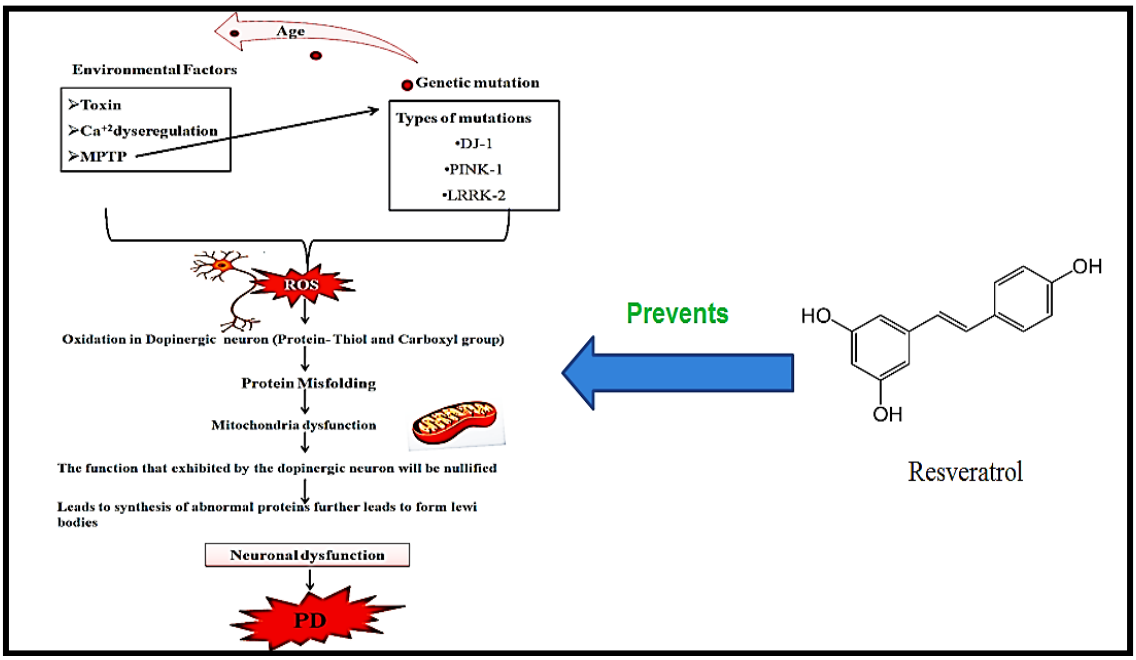

Figure 1: Illustration of the mechanism action of resveratrol

[4]. Different potential therapies based on nanoparticles and Nanosystems have explored various benefits. The science involved in nanotechnology is the creation of particles, materials, systems into nanometers.

At present nanotechnology is exposed to explosive advancement in many fields. Nanoparticles act as a transport vehicle for the delivery of medicine at specific sites. It has several benefits over other colloidal carrier systems, such as drug trapping, extended release of drugs, enhanced chemical and physical stability, and effective integration of lipophilic drugs. NPS was developed to regulate and protect the drug release from enzymatic and chemical degradation, thereby increasing its therapeutic efficacy. Nano lipid particles enhance the drug influx through the blood-brain barrier.

II. MATERIALS AND METHODS

Materials

The Phytochemical Resveratrol was obtained as a gift sample from Novel Nutrients Pvt. Ltd, Bengaluru, Karnataka India; whereas the liquid lipid Coconut oil was purchased from Mahavir coconut industries, Tumkur, Karnataka, India. The surfactant such as tween 80 obtain from LobaChemie, Mumbai, HPLC-grade ethanol was procured from Merck, Mumbai, The solid lipid stearic acid was purchased from Alpha Chemika, Mumbai.

Methods

Scanning for λ_{max} of Resveratrol

[5].UV visible spectrophotometric analysis of Resveratrol was carried out by using UV 1800 spectrophotometer. Spectrum was recorded in the range of 200 – 800 nm using ethanol as a solvent and its lambda max was recorded

Determination of λ_{max} and calibration of standard curve of Resveratrol by UV spectroscopy

Stock solution: 10mg of Resveratrol was accurately weighed and transferred to a 100mL volumetric flask. The Drug was then dissolved by adding in 80ml of ethanol by sonicating for 5min and volume was adjusted to 100ml to obtain a concentration of 100 µg/ml. An aliquot of 5 ml was transferred into 50 ml of volumetric flask. Volume was made up to 50 ml using ethanol to obtain a concentration of 10 µg/mL.

Standard curve: From the final stock solution aliquots of 2,4,6,8 mL was pipetted into a 10 mL volumetric flask to obtain concentrations ranging from 2- 10µg/mL and absorbances were obtained for each dilution. The concentration of each absorbance obtained was calculated and reported. A calibration curve was generated with the concentration on the x-axis and absorbance on the y-axis.

FTIR Studies

International Journal of Pharmaceutical Research and Applications
Volume 7, Issue 1 Jan-Feb 2022, pp: 961-987 www.ijprajournal.com ISSN: 2249-7781

[6]. FT-IR was used to determine the purity and compatibility of the drug. Interactions between drug and excipients can be analyzed by using Fourier Transform Infrared Analysis. The drug and excipient are triturated in mortar and pestle. The sample powder is dispersed in KBr powder at a ratio of 1:4 and is prepared by applying the pressure of 600 kg / cm2 in pellet form using the kbr pressed pellet technique. And for liquid lipid samples,a sodium chloride disc was used for spectral measurement, the resulting pellet is placed in a sample cell. The wavenumber is obtained from 4000 cm^{-1} to 400 cm^{-1} regions by diffusing the reflectance of the spectra powder on an FT-IR spectrophotometer.

Differential scanning calorimetry

[7,21]. DSC is a thermoanalytical procedure in which the heat difference required to increase the temperature of a sample is determined by the reference temperature. DSC technique is widely used to determine the melting point for either pure drugs or mixtures. The samples are pressed using shells made of aluminum. Calorimetric measurements of reference cells are made with an empty shell and calorimetric measurements of sample cells were made with compressing test compounds in the shell. Spectral measurements were collected at a temperature range of 20-265 ° C on DSC-60. DSC analysis calculates the energy that is consumed or released from a sample to provide endothermal and exothermic processes with quantitative and qualitative data. The energy was measured as J / Kcal.

Determination of log p by chem office software

[8]. The structure of the molecule was drawn in the Chem office, after a click on the option “analysis” Then it shows the chemical properties of the molecule.

Solubility

Saturation Shake-Flask Method

[9,10]. The shake flask technique was developed 40 years ago and still is considered the most reliable and widely used solubility measurement technique for solutions. It is typically produced by incorporating moderate amounts of solid to the solubility medium in a stoppered flask. There is a need for accurate measurement of the medium,As a result, the degree of solubility of the drug candidate can be estimated based on it. Although ensuring a sufficient quantity of added material to produce a suspension is important, it is therefore important that the added quantities of material will change the properties of the solution medium substantially, including its pH. So at the end of the test, the pH of the suspension should be checked. after adding every pinch of known concentrations of solids to the flask it was shaken or kept in a vortex shaker.

Screening of liquid lipids and surfactants

[11,12]. Different surfactants have been filtered in diverse concentrations by emulsifying experiment with lipid matrix, the degree of emulsification capacity of different surfactants was measured by this experiment. The lipid matrix with water and surfactants were taken in different mass ratios to examine its emulsifying capacity. Surfactants were blended with lipid matrix, resveratrol, and millipore water at 35 ° C for 10 min with 800 rpm,and then emulsion was subjected for cooling after its centrifugation. The surfactant with a good emulsifying effect was selected.

Screening of binary lipid phase

[13]. The highest miscibility of solid lipids with liquid lipids was determined by mixing different ratios of 95:5, 90:10, 70:30, and 60:40 of solid lipids and liquid lipids. The mixture was blended for 1 hour at 75 ºC at 300rpm with a magnetic stirrer. Miscibility is recognized by the sudden cooling on a filter paper to show any precipitation of a solid lipid. A binary mixture with a melting point greater than 40 ºC is selected by the absence of precipitation or recrystallization.

Screening of factors that are affecting the formulation

[14]. A factorial design is a computerized optimization technique to assess the importance of factors for the formulation of Resveratrol-loaded NLC. A 2 × 3 full factorial design is employed. Liquid lipid concentration, surfactant concentration, stirring speed were selected as factors to check their effects on Particle size, entrapment efficiency, and PDI.

Table 1: A factorial design for screening factors and their responses

International Journal of Pharmaceutical Research and Applications
Volume 7, Issue 1 Jan-Feb 2022, pp: 961-987 www.ijprajournal.com ISSN: 2249-7781

	Factor 1	Factor 2	Factor 3	Response 1	Response 2	Response 3
Run	A:Lipid Concentration (mg)	B:Surfactant Concentration (%)	C:Stirring Speed(rpm)	Particle Size	PDI	Entrapment Efficiency
	Mg	%	Rpm	nm		%
1	300	5	10000			
2	300	3	10000			
3	200	3	15000			
4	200	4	5000			
5	400	4	5000			
6	300	3	15000			
7	300	4	5000			
8	200	3	15000			
9	300	4	10000			
10	200	5	15000			
11	300	5	5000			
12	300	5	10000			
13	200	5	10000			
14	300	3	5000			
15	400	5	10000			
16	300	5	10000			
17	300	5	10000			

Formulation studies

Method of preparation

[15]. NLC preparation was carried out by the hot-melt homogenization method. The solid lipid was heated to a temperature above the melting point and the weighed amount of drug was added to which simultaneously liquid lipid was added and next co-surfactant ethanol was added, Aqueous phase containing the surfactant were also maintained at the same temperature as the molten lipid mixture. After attaining the same temperature, the lipid phase was added to the aqueous phase slowly under high-speed homogenization for 20 min at 15000 RPM. The solution obtained after homogenization was ultrasonicated for 15 min using a probe sonicator. NLCs were then cooled down to room temperature and lyophilized for long-term storage.

Optimization of formulation

[16]. To determine the effects of the independent variables on the dependent variables (particle size, PDI, and %EE), Box–Behnken design was used which have 17 run experiment with 5 center points, Box-Behnken (BBD) designs are a class of second-order designs, which are rotatable based on preliminary screening of the various factors that can affect the response, three independent variables were chosen. They are solid lipid to liquid lipid ratio, surfactant concentration, and homogenization speed. The interaction plots and polynomial equations that depict the interaction between factors and their special effects were created using computer design software. The sequential model sum of squares, lack of fit test, and model summary statistics were accountable for the selection of models for response analysis. The quadratic model selection for analysis of all the three responses was based on the Prob > F value of $P < 0.0001$, high R^2 value, low standard deviation, and the low value predicted residual error sum of the square are taken into consideration, the optimized formulation whose desirability is one or near one is selected.

Table 2: Variables in Box -Behnken design.

International Journal of Pharmaceutical Research and Applications
Volume 7, Issue 1 Jan-Feb 2022, pp: 961-987 www.ijprajournal.com ISSN: 2249-7781

Independent variables with their levels and dependent variables with their constraints for the preparation of Resveratrol NLCs

	Levels	
Variables	**Low (-1)**	**High (+1)**
Independent variables		
Lipid concentration (mg)	200	400
Surfactant concentration (%)	3	5
Homogenization speed (rpm)	5000	15000
Dependent variables		
Particle size (nm)	Minimize	
PDI	Minimize	
Entrapment efficiency (%)	Maximize	

Evaluation of NLC

Particle size, polydispersity index, and zeta potential

[17]. The particle size analysis and the charge of the prepared NLC were determined by Malvern zeta sizer (Malvern Instruments) at 25± 1°C. For the analysis, the samples were diluted to a 1:10 ratio with milli-Q water. Samples were transferred to a disposable polystyrene cuvette filled to 1cm depth. The analysis provided the average particle size and particle size distribution expressed as PDI (polydispersity index) which is ideal should be less than 1. For determining the charge of the formulation, it was performed using a clear disposable zeta cell, water as a dispersant which has a refractive index (RI) - 1.330 and viscosity (cP) - 0.88, and the temperature was kept constant at 25 °C. The sample was analyzed three times to minimize the error.

Entrapment efficiency

[12]. The entrapment efficiency of the prepared NLCs was estimated by centrifuging the formulations in the centrifuge machine (REMI cooling centrifuge). The formulations were centrifuged at 15000rpm for 30min at 4°C. The supernatant was appropriately diluted with Methanol for estimating the amount of free drug in the formulation. The entrapped drug and drug-loading capacity was quantified by the following equation:

$$\text{Entrapment efficiency \%} = \left[\frac{(\text{Total drug} - \text{drug in the supernatant})}{\text{Total drug}}\right] \text{x } 100$$

The diluted samples were then analyzed by UV which was connected with the UV detector. The mobile phase is comprised of ethanol and water.

Percentage yield

[2]. The freshly formulated NLC dispersions were lyophilized to produce dry samples for further studies such as structural analysis, The dispersion had pre-frozen for 4 h at -50 ° C. Then, a vapor condenser (-80 ° C) and a vacuum pump (< 0,1 Torr) dried the frozen samples for 24 h. NLC powders were collected after lyophilization and stored in the glass vial at room temperature for structural analysis, before lyophilization, no cryoprotectants were added to the dispersions since the analysis of particle structure was impressionable.

Percentage yield is calculated using the weight of the nanoparticles obtained after lyophilization

The formulae used to calculate the percentage yield is

$$\text{percentage yield} = \frac{\text{weight of nanoparticles obtained}}{\text{Total weight of lipid and drug}} \times 100$$

International Journal of Pharmaceutical Research and Applications
Volume 7, Issue 1 Jan-Feb 2022, pp: 961-987 www.ijprajournal.com ISSN: 2249-7781

Characterization of NLCS

Scanning electron microscope (SEM)

[18]. Using the gold sputter technique, a scanning electron microscope was utilized to characterize the shape and surface of the NLC formulations, the formulation was poured into an aluminum stub on a two-sided tape, the stubs were gold-coated and 400A^{o} thick. A pressure of 0.6mmHg is maintained in the chamber while the photograph is taken with a voltage of 20Kv.

In vitro release studies

[11,12,19]. In vitro drug release from NLC was performed using the dialysis bag method.

The phosphate buffer saline buffer (pH 7.2) was chosen as the receptor medium to achieve sink conditions. At a magnetic stirring of 250 rpm and 37 ± 0.5 ° C, the dialysis bag containing a 2 mL sample was immersed in the receptor medium (200 mL). Before the drug release study, the dialysis membrane was pretreated by soaking it for 12 h in the receptor medium; this is called Activation of a membrane to facilitate its pore opening. At defined intervals of time (0, 2, 4, 6, 12, 24, 48, 72, 96) 1 ml of the receptor medium was withdrawn for analysis. And immediately refilled with an equal volume of semi-warmed receptor medium to maintain sink conditions.

Stability studies

[12,22]. The studies were carried out for the optimized prepared NLC. The optimized formulation was packed ina 10mL/20mm vial with coated and uncoated stoppers and the formulation is stored at 25^{o}C/60% RH, 40^{o}C/75% RH And the formulation was checked for particle size, PDI, Zeta Potential.

III. RESULTS

Preformulation

Analysis

Determination of lambda max (λmax) of Resveratrol

The λmax of pure resveratrol was found out by scanning 10 microgram/ml solution in UV-Visible range which are 200 – 800 nm and the λmax was found at 305nm with the absorbance of 0.752. The UV Spectroscopy graph of Resveratrol was shown in Figure 2.

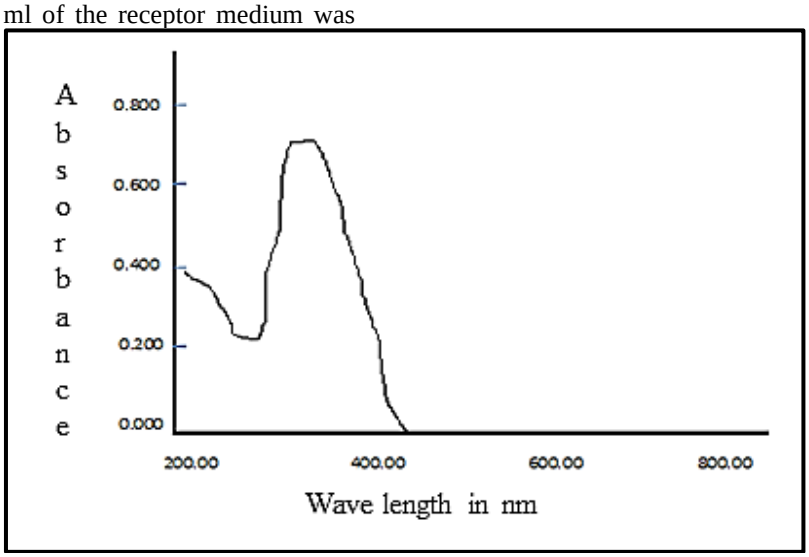

Figure 2: UV Spectroscopy graph

Standard calibration curve of Resveratrol

From the stock solution of 10µg/ml, further dilutions were made to obtain the solution with a concentration of 2,4,6,8 µg/ml of resveratrol solution [22]. At photometric mode, the absorbance of resveratrol solution with 2µg/ml and remaining concentrations was measured at 305nm. The standard calibration curve graph was shown in Figure 3.

Table 3: Accuracy values of standard calibration curve of Resveratrol

International Journal of Pharmaceutical Research and Applications
Volume 7, Issue 1 Jan-Feb 2022, pp: 961-987 www.ijprajournal.com ISSN: 2249-7781

S.No	Concentration µg/ml	Absorbance (305nm)
1	0	0
2	2	0.094
3	4	0.276
4	6	0.418
5	8	0.580
6	10	0.754

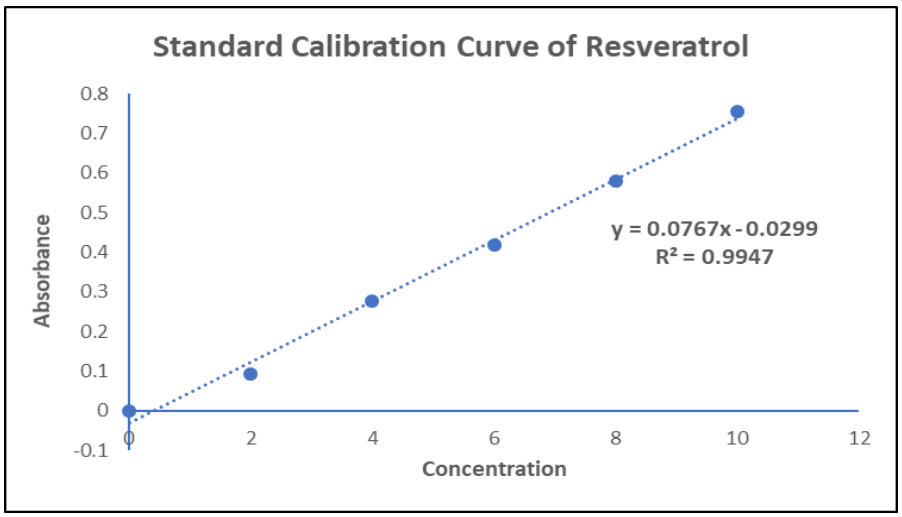

Figure 3: Typical standard calibration curve graph

FTIR

FTIR measurements can provide very important information about the functional groups present in the drug molecule.

Resveratrol: Peak at 3263cm^{-1}indicates the presence of OH group, peaks at 2055- 2166 cm^{-1} corresponds to symmetric bonds (C-C=C-C), peak at 1508 cm^{-1} corresponds to alkene group (C=C), peak at 1383-1427 cm^{-1} corresponds to CH_2 group, and peak at 1585 cm^{-1} corresponds to aromatic rings. The FTIR graph of Resveratrol was shown in Figure 4.

International Journal of Pharmaceutical Research and Applications
Volume 7, Issue 1 Jan-Feb 2022, pp: 961-987 www.ijprajournal.com ISSN: 2249-7781

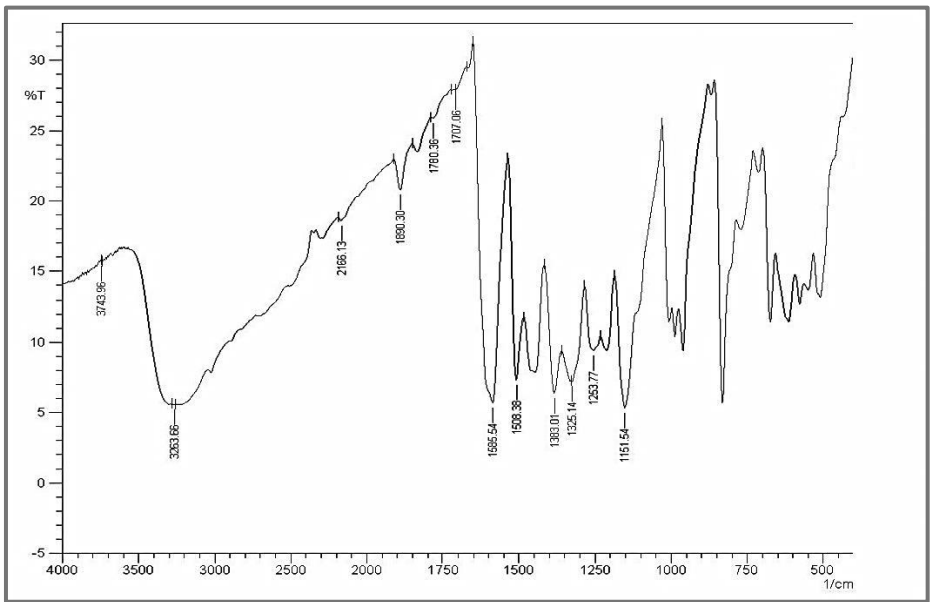

Figure 4: FTIR of Resveratrol

DSC (Differential scanning calorimeter)

DSC of Resveratrol was performed by DSC 60 instrument.

The melting point of Resveratrol was determined by DSC studies and the thermograms are presented below

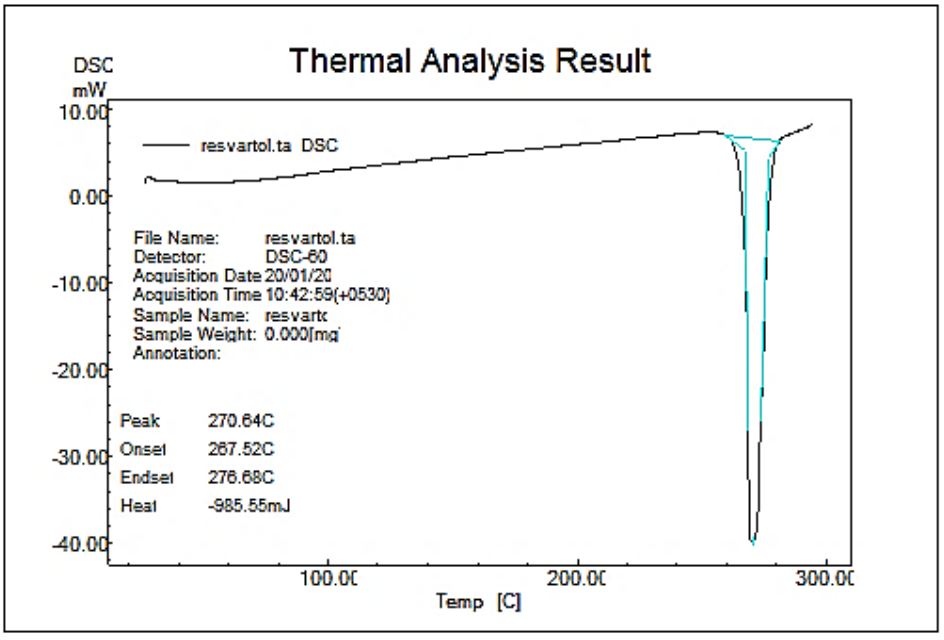

Figure 5: DSC Thermogram of Resveratrol

Determination of log p by chem office software

Across many areas, ChemDraw has continually expanded, becoming the leading and quick approach for the exploration of chemistry.

3D ChemDraw is the most popular program for modeling chemistry molecules, and to know the properties of molecules.

The log p-value of resveratrol was **3.06** which was shown in figure 6.

International Journal of Pharmaceutical Research and Applications
Volume 7, Issue 1 Jan-Feb 2022, pp: 961-987 www.ijprajournal.com ISSN: 2249-7781

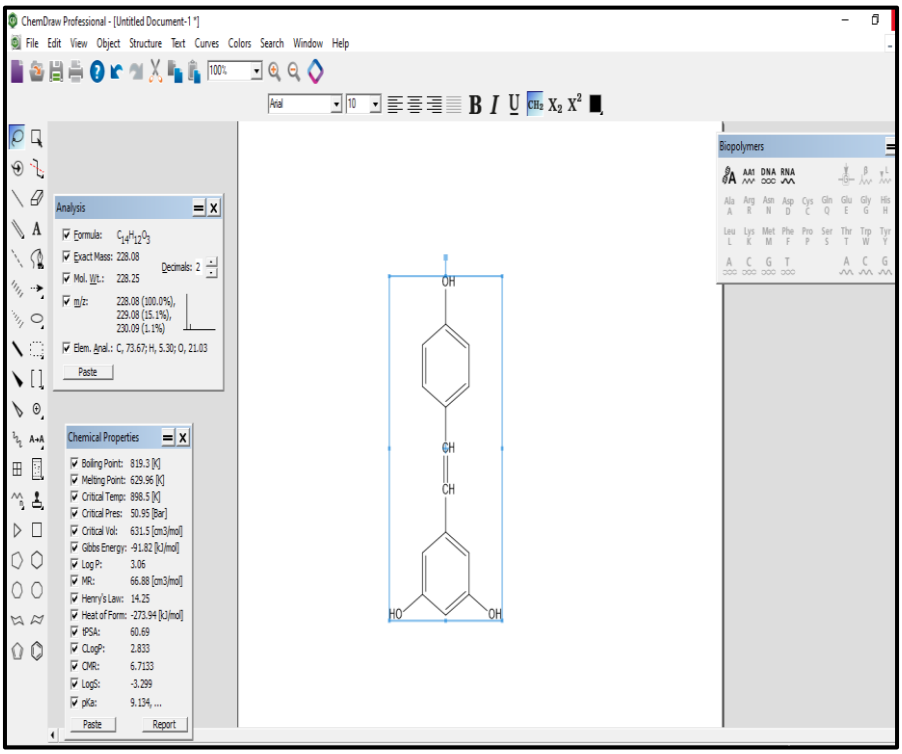

Figure 6: Demonstration of log p-value by chem office software

Solubility studies

To the known quantity of solvent 1mg of the drug was added, once it gets dissolved further known quantity of the drug was frequently added until it becomes a supersaturated solution, the process was continued by vortexing after every addition and it is continued until the drug stopped dissolving in the solvent. Now it is subjected to filtration and the undissolved solids in Whatman filter paper were dried and weighed.

Solubility: The solubility of Resveratrol was highest in ethanol, methanol with a solubility of12±0.5mg/ml. The least solubility of resveratrol was observed in water.

Table 4: Results of solubility analysis

S.NO	Sample	Solvent	Concentration mg/ml	Descriptive term
1	Resveratrol	Methanol	35± 2 in 0.5ml	Soluble
2	Resveratrol	Ethanol	53 ± 1 in 0.5 ml	Freely Soluble
3	Resveratrol	Water	0.1mg in 1ml	very slightly soluble
4	Resveratrol	Oleic acid	< 0.1 mg in 1ml	Insoluble
5	Resveratrol	Tocopherol	6mg in 0.5ml	sparingly soluble
6	Resveratrol	Coconut oil	16 ± 2mg in 0.5ml	Soluble
7	Resveratrol	Soya bean oil	4 ± 2mg in 0.5 ml	sparingly soluble
8	Resveratrol	Stearic acid	5 ± 1mg in 0.5 ml	sparingly soluble
9	Resveratrol	Campritol	2 ± 1mg in 0.5 ml	slightly soluble
10	Resveratrol	Tween 80	12± 2mg in 0.5ml	sparingly soluble
11	Resveratrol	1.2 Hcl buffer	48 ± 2mg in 0.5ml	Freely Soluble

Screening of lipids

[11]. The screening of a binary mixture of lipids was done based on the solubility of Resveratrol and the compatibility profile of resveratrol on different solid and liquid lipids. Initially, resveratrol solubility has been examined in various combinations of solid and liquid lipids. Analysis of lipids and their dissolving potentials.

International Journal of Pharmaceutical Research and Applications
Volume 7, Issue 1 Jan-Feb 2022, pp: 961-987 www.ijprajournal.com ISSN: 2249-7781

(+, dissolved under heating;
-not dissolved under heating ±dissolved under heat but recrystallization).

Table 5: Solubility profile and crystallinity of the drug in various combinations of liquid lipids and solid lipids

Liquid lipid	Solid lipid	Resveratrol		
		2mg	4mg	6mg
Coconut oil	Glyceryl monostearate	+	±	±
Coconut oil	Campritol	±	-	-
Coconut oil	Stearic acid	+	+	±
Soybean oil	Campritol	-	-	-
Soybean oil	Lauric acid	-	-	-
Soybean oil	Glyceryl monostearate	+	±	±
Oleic acid	Campritol	±	-	-

Surfactant screening

[12]. The solubility of resveratrol and the emulsification nature of different surfactants in different liquid lipids with water was determined after centrifugation.

Table 6: Screening report for selection of best suitable surfactant

SURFACTANT	**SURFACTANT CONCENTRATION**		
	1.5	2	3
Tween 80	-	+	++
Tween 60	-	-	-
Tween 20	-	-	+
Span 20	-	-	-

Assessment of surfactants and outcomes of the emulsifying test results (- indicates gelation or oil separation during cooling and after centrifugation test ++ indicates no oil separation + indicates oil separation)

[23]. Based on the above results Tween 80 was selected as a surfactant for the formulation, and another reason for the selection of tween 80 is it was scientifically proved that polysorbate coated nanoparticles especially Tween 80, will be able to transport the loaded drugs via BBB to C.N.S after administration. So, for brain targeting nanoparticles tween 80 act as a transporter for crossing the blood-brain barrier.

Compatibility study of Coconut oiland Resveratrol by FTIR

[24]. Based on the solubility profile of the drug in a different mixture of lipids the following combination of lipids was selected for formulations and the Compatibility studies of those with the drug was determined by FTIR, the drug was mixed thoroughly with coconut oil in a ratio of 1:3 the samples are kept aside for one week after the sample was subjected to FTIR studies.The functional groups present in resveratrol are not reacted with coconut oil and hence the peaks that it exhibits remain the same with functional groups of its excipient, thereby, it is compatible with coconut oil.

International Journal of Pharmaceutical Research and Applications
Volume 7, Issue 1 Jan-Feb 2022, pp: 961-987 www.ijprajournal.com ISSN: 2249-7781

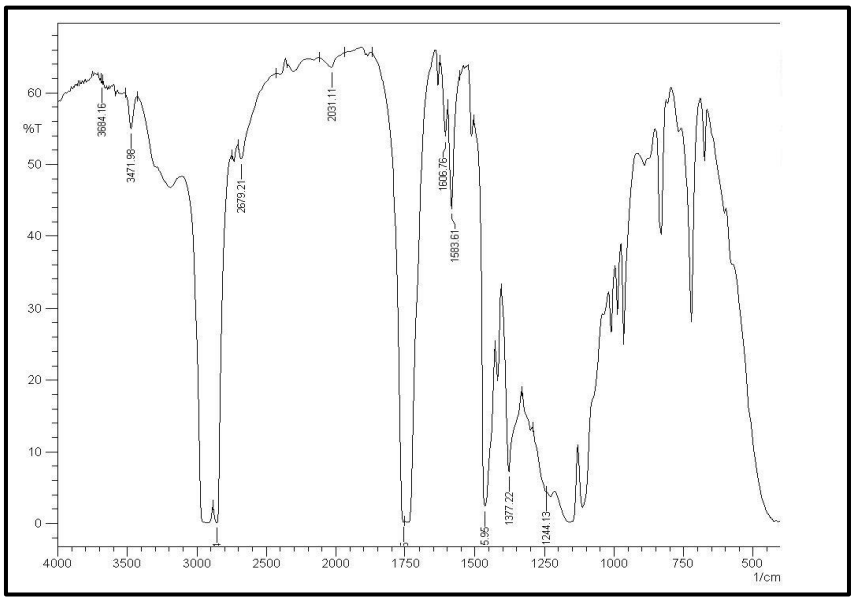

Figure 7: Compatability report of coconut oil and resveratrol

Compatibility study of Stearic acid and Resveratrol by DSC

There is no change in endothermic peaks of resveratrol when it is combined with stearic acid, and hence it is concluded that there are no incompatibility issues.

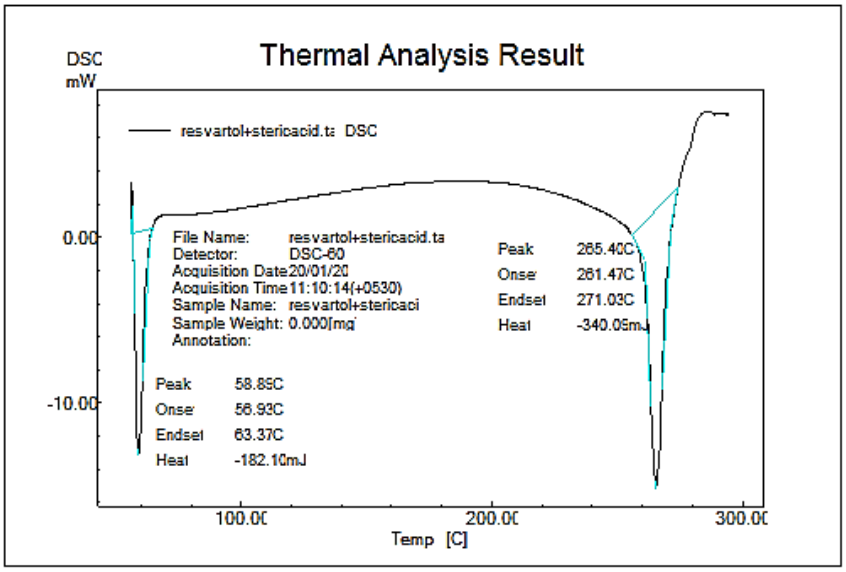

Figure 8: compatibility report of resveratrol and stearic acid by DSC

Screening of binary lipid phase

[25]. The solid and liquid lipid selected for the formulation was observed to be miscible in the ratio of 95:5, 95:10, 70:30, and 60:40.

International Journal of Pharmaceutical Research and Applications
Volume 7, Issue 1 Jan-Feb 2022, pp: 961-987 www.ijprajournal.com ISSN: 2249-7781

Table 7: The miscibility report of solid and liquid lipids in different ratio

S.NO	Solid lipid: liquid lipid	Miscibility
1	95:5	++
2	90:10	++
3	70:30	++
4	60:40	++

++ indicates miscibility

Screening of NLC base for Resveratrol and optimization by Box-Behnken design

[12]. NLCs were prepared by taking the solid lipid, liquid lipids which have the highest solubility, and the surfactant with the highest emulsifying capacity in lower concentrations. Thus, the components selected for the formulation were coconut oil, stearic acid as lipids and Tween 80 as a surfactant, ethanol as co-surfactant. NLC was prepared using hot melt homogenization as the method of preparation. Initially, the concentration of the components was blindly selected and the formulations were analyzed for any incompatibility based on their physical appearance. and other characterization results, most of the formulations showed phase separation in various concentrations so this information will help to set up the limits for selection of a concentration of excipients during the preparation thus it concludes failed formulations will promote the selection of appropriate concentrations of excipients to get better, best formulations for the study and finally the formulation was optimized by Using Box- Behnken design.

Observed responses for Resveratrol NLC

Table 8: Results of NLC formulations upon different factors

	Factor 1	Factor 2	Factor 3	Response 1	Response 2s	Response 3
Run	A:Lipid Concentration (mg)	B: Surfactant Concentration (%)	C:Strirring Speed(rpm)	Particle Size	PDI	Entrapment Efficiency
	Mg	%	Rpm	nm		%
1	300	5	10000	246	0.322	78
2	300	3	10000	210	0.433	77
3	200	3	15000	184	0.388	72
4	200	4	5000	367	0.654	73
5	400	4	5000	435	0.588	78.3
6	300	3	15000	162	0.394	79
7	300	4	5000	150	0.401	74
8	200	3	15000	79	0.247	73
9	300	4	10000	128	0.329	74.3
10	200	5	15000	74	0.234	68
11	300	5	5000	128	0.327	74.2
12	300	5	10000	247	0.326	74.3
13	200	5	10000	82	0.217	68
14	300	3	5000	532	0.687	81
15	400	5	10000	446	0.693	83
16	300	5	10000	241	0.351	67
17	300	5	10000	239	0.348	69

International Journal of Pharmaceutical Research and Applications
Volume 7, Issue 1 Jan-Feb 2022, pp: 961-987 www.ijprajournal.com ISSN: 2249-7781

Mathematical models for the design of experiments

Screening of Resveratrol formulation

The full factorial design had generated 17 experimental runs for formulation development. The values of the responses -particle size (R1), PDI (R2), and entrapment efficiency (R3) were recorded. The particle size of the formulations fell into the range of 74 to 532 PDI in the range of 0.217to 0.693 and entrapment efficiency in the range of 68 to 83. The 3D response graphs of Particle size, PDI, and Entrapment efficiency were shown in Figures 9, 10,11.

The final equation in coded-factor terminology

Table 9: Coded factors of Particle size

Particle size (R1)	=
+242.19	
+127.05	A
-30.71	B
-31.66	C

Table 10: Coded factors of PDI

PDI (R2)	=
+0.3417	
+0.0953	A
-0.0775	B
-0.0619	C
+0.0400	AB
+0.1146	AC
+0.0640	BC
+0.1214	A^2
+0.0214	B^2
+0.0583	C^2

Table 11: Coded factors of Entrapment efficiency

Entrapment efficiency (R3)	=
+76.87	
+3.67	A
-2.21	B
+0.1246	C
+1.21	AB
+2.83	AC
+0.6274	BC

International Journal of Pharmaceutical Research and Applications
Volume 7, Issue 1 Jan-Feb 2022, pp: 961-987 www.ijprajournal.com ISSN: 2249-7781

The Effects plots for the responses are as follows:

Particle size

Analysis of response using a 3D Surface graph.

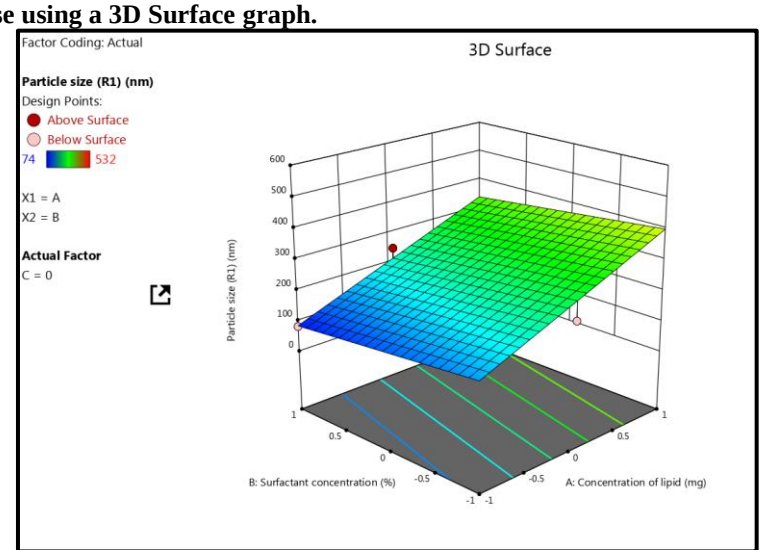

Figure 9: illustration of 3D response graph of particle size

The final equation from table 9 determines the effect of each factor on the particle size. The "+" sign indicates a positive effect and the "-" sign indicates a negative effect, As per fig 9, the blue color suggests the lowest value of particle size, the green color indicates the highest value of particle size, therefore the slight increase in lipid concentration with simultaneous decreasing in surfactant concentration and homogenization speed will increase the particle size.

P.D.I

Analysis of response using a 3D Surface graph.

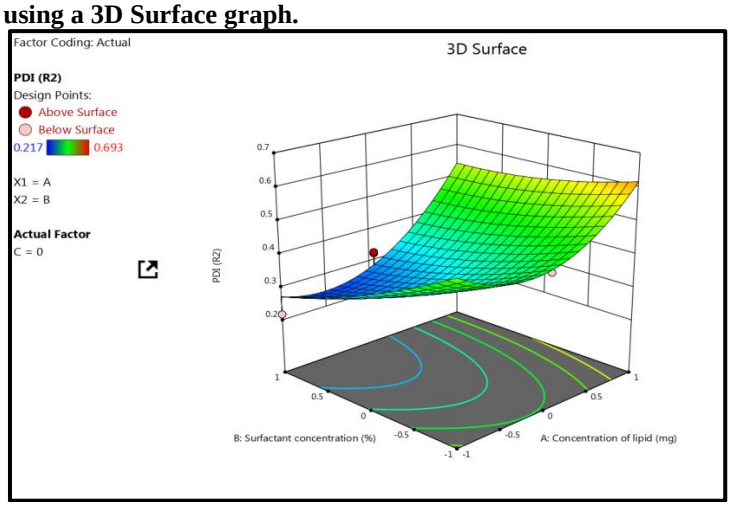

Figure 10: illustration of 3D response graph of PDI

The final equation from table 10 and as per fig 15, the blue color suggests the lowest value of PDI, the red color indicates the highest value of PDI, therefore the slight increase in lipid concentration with simultaneous decreasing in the surfactant concentration will increase the Particle size distribution.

International Journal of Pharmaceutical Research and Applications
Volume 7, Issue 1 Jan-Feb 2022, pp: 961-987 www.ijprajournal.com ISSN: 2249-7781

Entrapment Efficiency

Analysis of response using a 3D Surface graph.

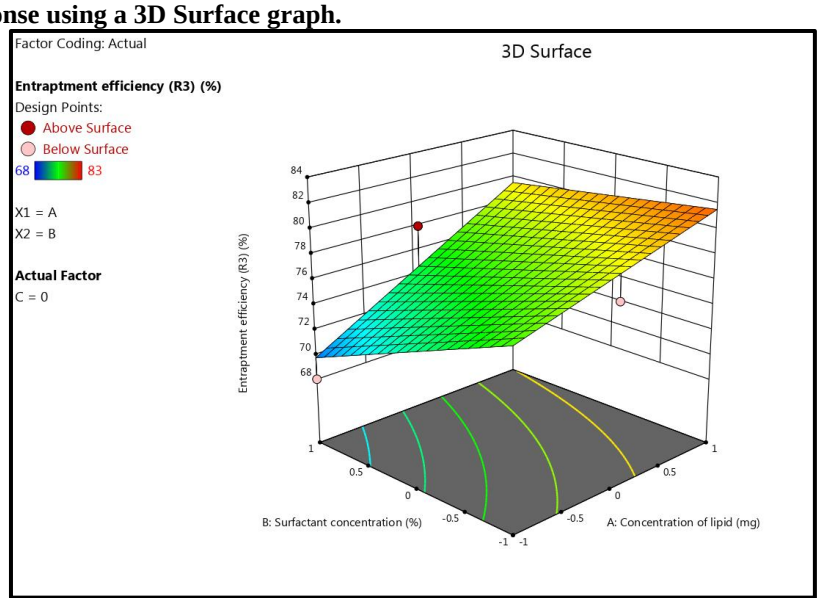

Figure 11: illustration of 3D response graph of Entrapment Efficiency

The final equation from table 11 and as per fig 11 the blue color indicates the lowest value of Entrapment efficiency, the red color suggests the highest value of Entrapment efficiency, therefore the slight increase in lipid concentration with the simultaneous increase in surfactant will increase the Entrapment efficiency

Screening of factors using design expert software

[26]. The factors like the concentration of lipid, the concentration of surfactant homogenization speed were selected for screening, these factors were found to be significant and it's effecting responses like particle size, entrapment efficiency, PDI. **R_2** values were less than 0.2.

The Table shows the significance of factors on the responses and the difference between predicted R_2 and adjusted R_2.

Table 12: significant values of predicted $R_2$and adjusted R_2

S.No	Factor	Effect on Z avg PDI and EE	Difference between predicted R_2 and adjusted R_2
1	Lipid	Significant	Less than 0.2
2	Surfactant	Significant	Less than 0.2
3	Speed	Significant	Less than 0.2

Preparation of Resveratrol loaded NLC

After generation of design space in DOE Software, the interrelation of input variables were easily identified and the desired output of NLC was achieved from the corresponding material attributes and process parameters, the optimized selected formulation in the table below has a desirability of 0.97

International Journal of Pharmaceutical Research and Applications
Volume 7, Issue 1 Jan-Feb 2022, pp: 961-987 www.ijprajournal.com ISSN: 2249-7781

Table 13: The optimized final formulation results

Factors	Liquid Lipid	Solid Lipid	Surfactant	Water + Cosurfactant	Homogenization		Sonication	
					Speed	Time	APT	Time
	100 mg	200 mg	0.48ml	8.5 +3ml	15000	10	40	20
Actual Response	**Particle Size** 126		**PDI** 0.327		**% EE** 70			

Evaluation Studies

Particle size, Zeta potential, PDI

[27]. The optimized two formulations of NLC with Z average were found to be 126 and 79. The graph shows a single peak with 100% intensity. The PDI of Resveratrol Nano formulation was found to be 0.327 and 0.247, the zeta potential of samples was found to be -27.6mV the results of zeta potential of the sample were above +30 and - 30 which indicates that the sample was stable, and PDI of 0.3 and below is considered to be acceptable, The Particle Size graph of Resveratrol NLC formulation was shown in Figure 12,13. The Zeta Potential of Resveratrol NLC was shown in Figure 14.

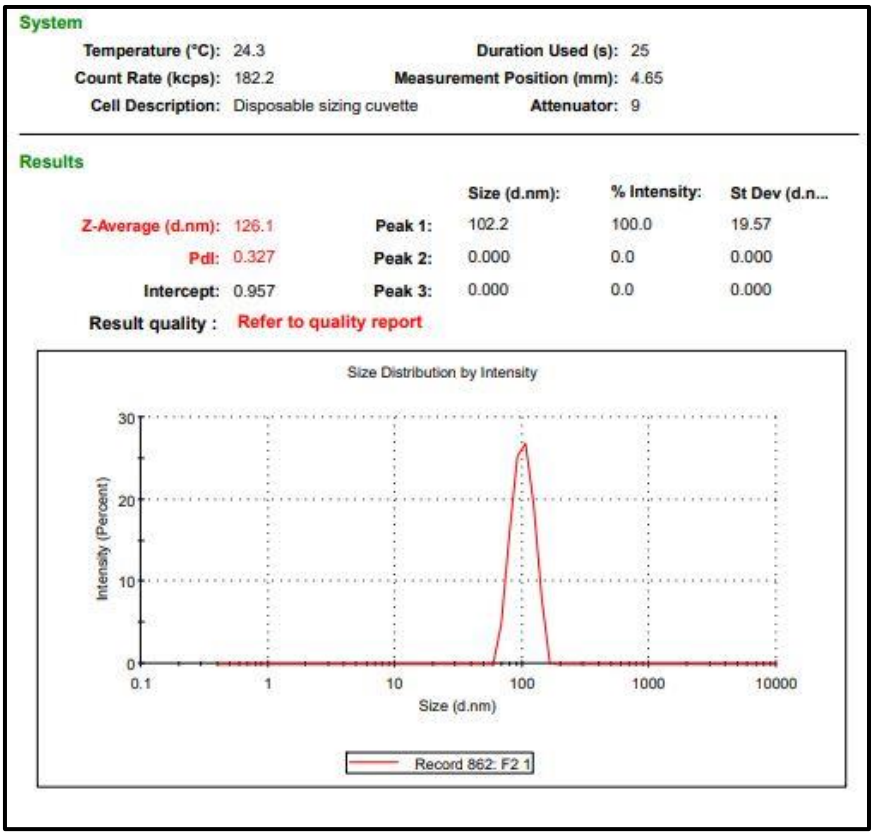

Figure 12: Particle size of optimized RES NLC

International Journal of Pharmaceutical Research and Applications
Volume 7, Issue 1 Jan-Feb 2022, pp: 961-987 www.ijprajournal.com ISSN: 2249-7781

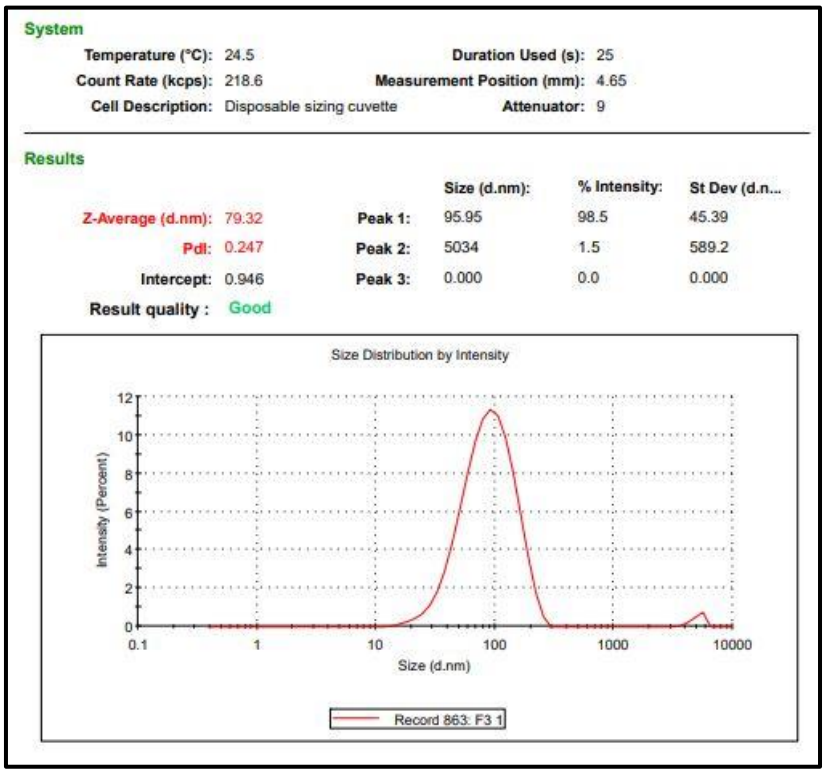

Figure 13: Particle size of optimized RES NLC

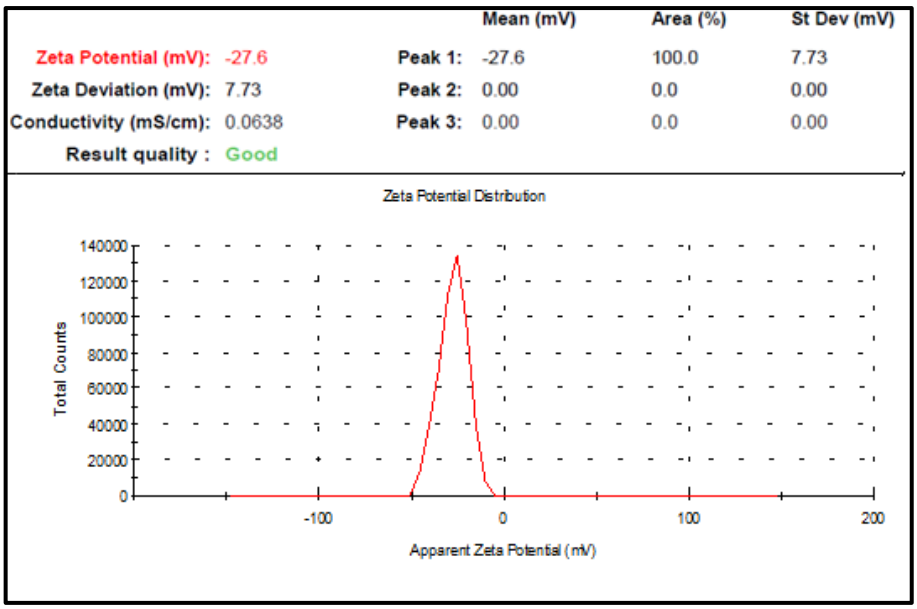

Figure 14: Zeta potential of optimized RES NLC

Entrapment efficiency

[12,28]. The entrapment efficiency of the prepared NLCs was estimated by centrifuging the formulations in the centrifuge machine. After centrifugation, the supernatant was collected and filtered through a 0.2 µm syringe filter, later it is appropriately diluted with ethanol for estimating the amount of free drug in the formulation. The entrapped efficiency was quantified by the following equation:

International Journal of Pharmaceutical Research and Applications
Volume 7, Issue 1 Jan-Feb 2022, pp: 961-987 www.ijprajournal.com ISSN: 2249-7781

$$\text{Entrapment efficiency \%} = \left[\frac{(\text{Total drug} - \text{drug in the supernatant})}{\text{Total drug}}\right] \text{x } 100$$

The entrapment efficiency of optimized formulae

$$\text{Entrapment efficiency \%} = \frac{200 - 59}{200} \times 100$$

Entrapment efficiency % = 70.2

Screening of Drug loading by FTIR

[29]. The Lyophilized NLC formulation was subjected for FTIR Studies the graph below shows there are no peaks related to functional groups of resveratrol hence it indicates the drug was completely entrapped in the lipid core. The FTIR graph of the Lyophilized formulation was shown in Figure 15.

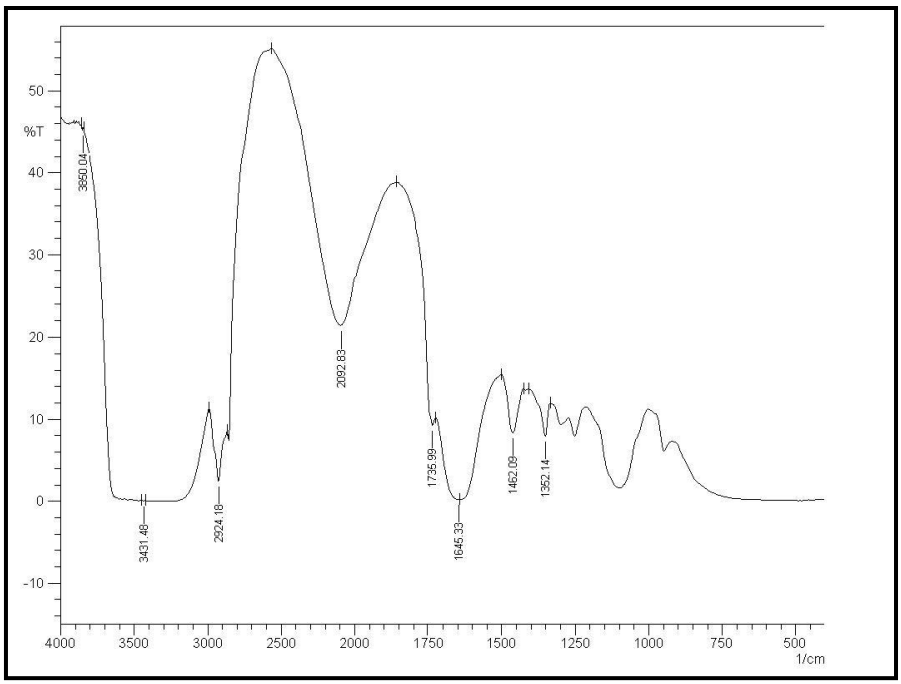

Figure 15: FTIR graph of the lyophilized formulation

Percentage yield

[2]. The weight of the lyophilized sample of Resveratrol was found to be 290 mg. The percentage Yield of Resveratrol was found to be 72.5.

$$\text{Percentage yield} = \frac{\text{weight of nanoparticles obtained}}{\text{Total weight of lipid and drug}} \times 100$$

$$\text{\% yield} = \frac{290}{400} \times 100$$

% Yield = **72.5**

SEM (Scanning electron microscope)

[28]. ZEISS SEM analysis was performed to determine the morphology of resveratrol-loaded lipid nanoparticles, the images illustrate that the resveratrol-loaded NLCs are almost spherical and uniform with smooth surfaces. SEM is the simplest visual method to obtain information on particulate surface morphology. And there had been no visible aggregation of particles. Moreover, resveratrol does not seem to be associated

International Journal of Pharmaceutical Research and Applications
Volume 7, Issue 1 Jan-Feb 2022, pp: 961-987 www.ijprajournal.com ISSN: 2249-7781

with morphological alterations or crystal formation. The SEM image of the NLC formulation was shown in Figure 16.

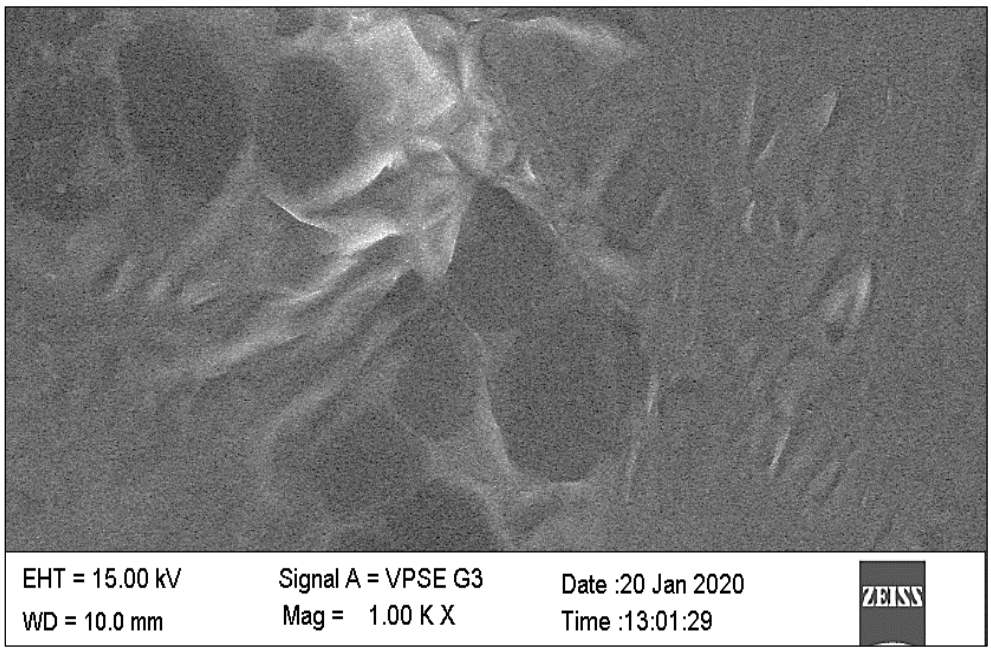

Figure 16: Scanning electron microscopic view of NLC formulation

In vitro release studies

[11,12,20]. The formulation of Resveratrol-loaded NLC was carried out for in vitro studies, The release of Resveratrol was recorded from 0 to 96th hr. depending upon the results; the data was used to select the best-fitting model. The graphical representation of various models was shown in Figures17,18,19,20,21.After assessing the in-vitro drug release it was concluded that release of drug follows Zero-order kinetics, and the Higuchi model indicated that the release of the drug from nanoparticles was through the diffusion process.

Table 14: cumulative % drug release values of resveratrol

Time (hr)	Cumulative % Drug Release
0	0.00
2	2.42
4	9.67
6	22.32
12	34.57
24	49.81
48	62.13
72	70.11
96	74.79

International Journal of Pharmaceutical Research and Applications
Volume 7, Issue 1 Jan-Feb 2022, pp: 961-987 www.ijprajournal.com ISSN: 2249-7781

Table 15: log cumulative % drug release values

Time	Log cumulative % to be released
0	1.21
2	1.52
4	1.46
6	1.42
12	1.36
24	1.30
48	1.23
72	1.19
96	1.16

In-vitro release studies following First order kinetics

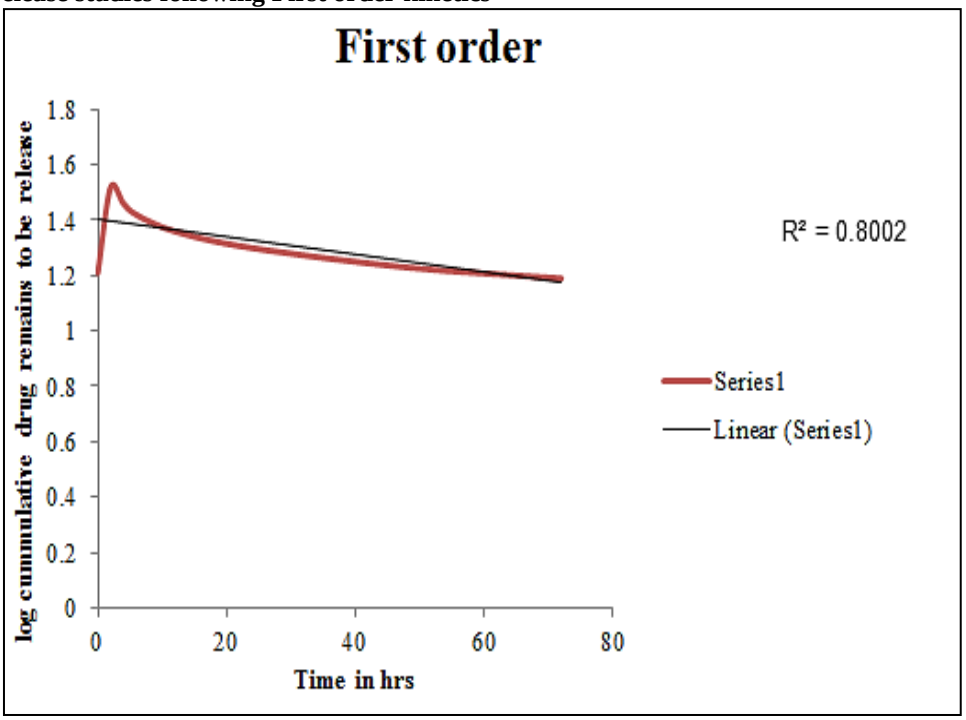

Figure 17: graphical representation of log cumulative % release

International Journal of Pharmaceutical Research and Applications
Volume 7, Issue 1 Jan-Feb 2022, pp: 961-987 www.ijprajournal.com ISSN: 2249-7781

Figure 18: graphical representation of log cumulative % release

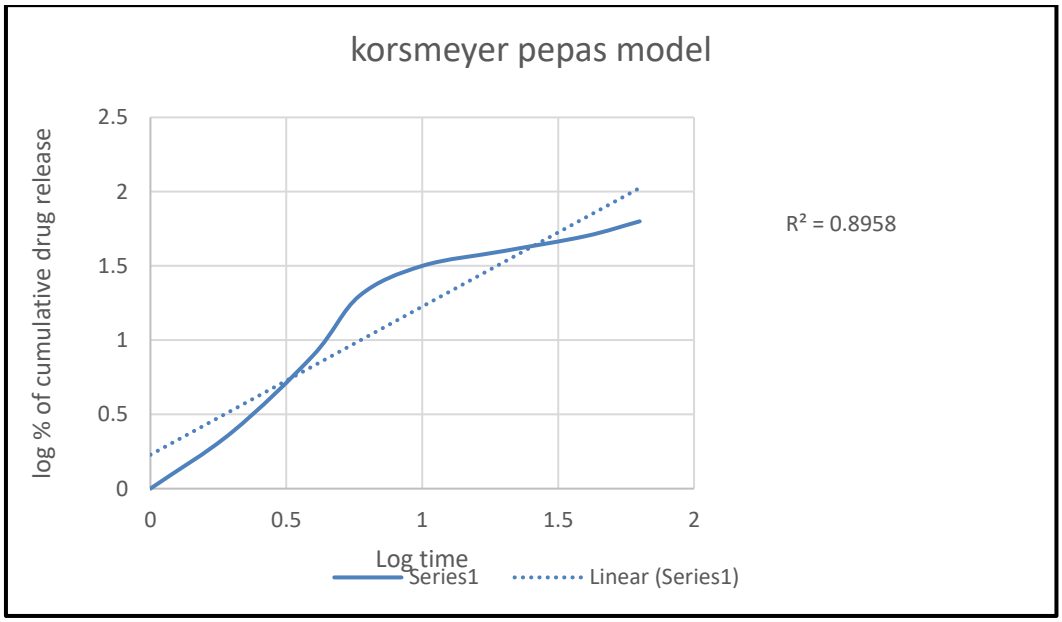

Figure 19: graphical representation of log cumulative % release

International Journal of Pharmaceutical Research and Applications
Volume 7, Issue 1 Jan-Feb 2022, pp: 961-987 www.ijprajournal.com ISSN: 2249-7781

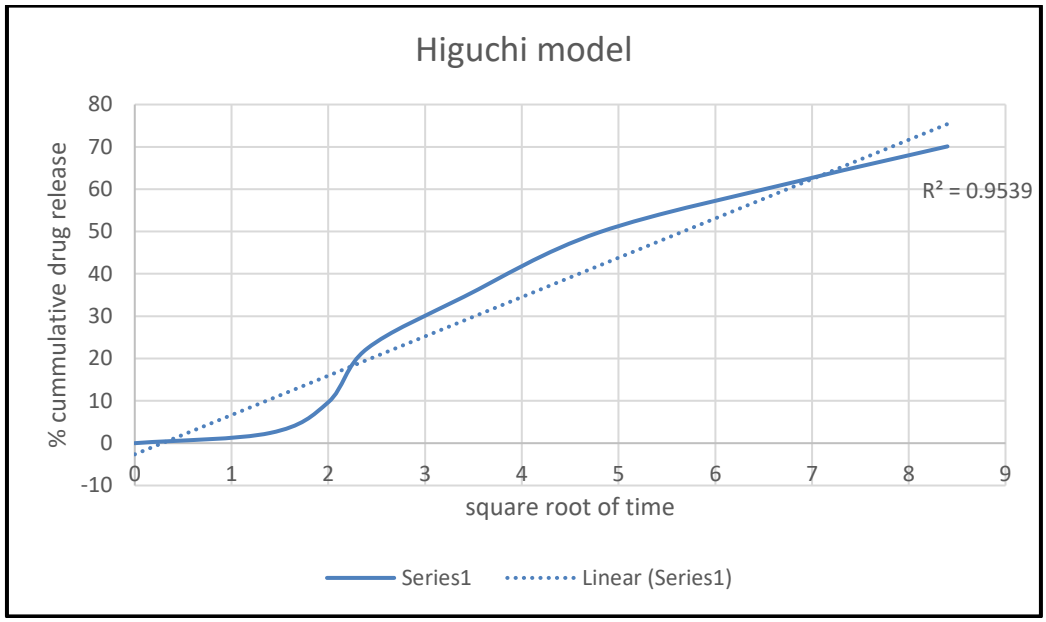

Figure 20: graphical representation of log cumulative % release

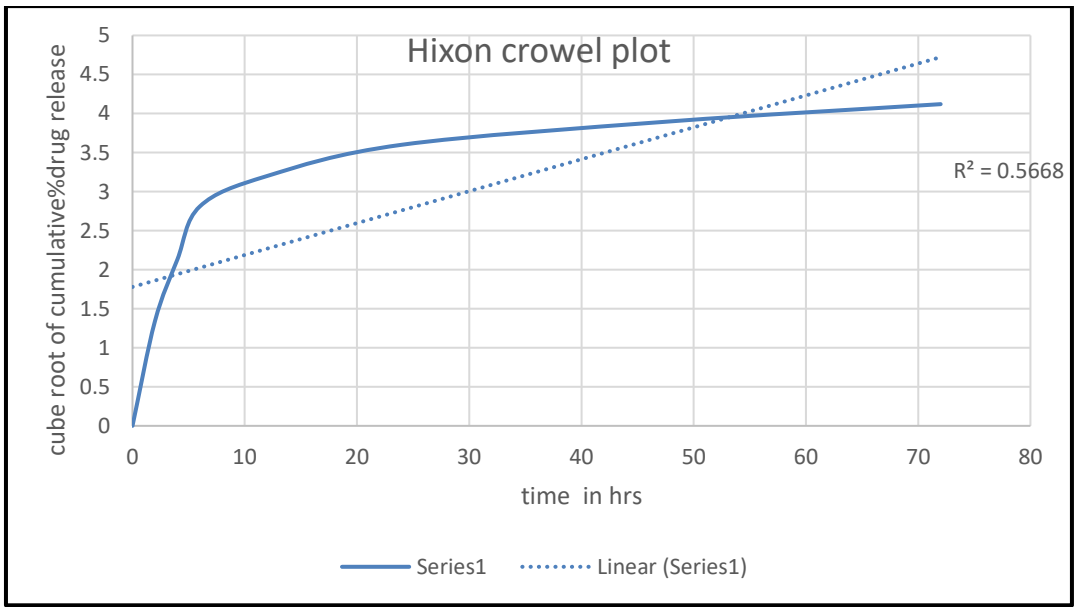

Figure 21: graphical representation of log cumulative % release

International Journal of Pharmaceutical Research and Applications
Volume 7, Issue 1 Jan-Feb 2022, pp: 961-987 www.ijprajournal.com ISSN: 2249-7781

Figure 22: Image illustrates in vitro drug release studies

Stability studies

[12,22]. The stability of the prepared formulation was checked at 25ºC/60%RH, 40ºC/75% RH, testing frequency was given for every 15 days, the formulation was filled in two types of stoppered vials and loaded in stability chamber. There was no drastic change in the particle size, PDI, and Zeta potential after storing the optimized formulation in different temperatures up to 30 days, after checking the stability in 45 the day the formulation was present in the coated stoppered vial at storage condition at 40ºC/75% RHwasunstable, particle size and PDI were completely changed. And remaining are in stable condition, after 60th day minor changes in Particle size and PDI were observed in the uncoated stoppered vial at 40ºC/75% RH, the formulation at 25ºC condition showed good stability in uncoated stoppered up to 90 days and after minor changes in PDI and Zeta potential was observed. Image of the unstable formulation after the 45$^{th\ day}$ was shown in Figure 23.

Figure 23: Image of the unstable formulation after 45$^{th\ day}$

IV. DISCUSSION

Pre-formulation studies

Recognition of appropriate excipients for the preparation of the formulation

Analysis of λmax of Resveratrol:

The λ_{max} of the drug was identified from the spectrum; the λ_{max} of the drug is identified as 304 nm.

International Journal of Pharmaceutical Research and Applications
Volume 7, Issue 1 Jan-Feb 2022, pp: 961-987 www.ijprajournal.com ISSN: 2249-7781

Standard calibration curve for Resveratrol:
It was observed that from the table the standard calibration curve, the drug obeys beer's law, and the result was found in the area of 2 - 10 µgm/mL in ethanol.

Solubility:
The solubility of Resveratrol was examined in various solvents, Resveratrol is partially soluble in water and the highest solubility is found in methanol, ethanol. The increasing order of Resveratrol solubility is as follows Ethanol> methanol>1.2 Hcl buffer solution > Tween 80 > Coconut oil > water.

FTIR:
The functional groups of the drug and compatibility of the drug with its excipients are estimated by the nujol null technique and the KBR pressed pellet technique. In order to study drug excipient compatibility, the IR spectrum of the combination of drug excipient mixture is compared to the IR spectrum of pure A.P.I and finally there no interactions are observed between the drug and selected excipients.

DSC:
Sample cells are prepared by placing traces amount of the sample in the aluminum shell and compressing them after placing the cap. The compressed cells are placed in the chamber and the melting point was measured to detect the effects of excipients on the melting point of the drug. From the readings, the drug was found to have no interactions with excipients.

Method of Preparation of Optimized Formulation:
This formulation was prepared by dissolving 3mg of a drug in solid lipid by the application of heat to which simultaneously liquid lipid was added and next 3ml of co-surfactant ethanol was added, an aqueous phase containing the surfactant(s) were also maintained at the same temperature as the molten lipid mixture. The oil phase was slowly transferred to the aqueous phase after achieving the same temperature under high-speed homogenization for 20 min at 15000 RPM. The solution obtained after homogenization was ultrasonicated for 15 min by using a probe sonicator

Design of Experiment:
The upper-lower limits of concentration of lipid and surfactant are obtained by the trial and error method. The values were incorporated into the 2×3factorial design. In this design, the effect of all the individual variables combination when each variable is tested at the highest and lowest level was analyzed. The factors affecting the responses significantly were taken into consideration for optimization. On these charts, the reference line (t-Value limit) is significant statistically. For particle size, PDI, EE the P-value was less than 0.05, therefore, it indicates the selected quadratic model was significant

3Dgraphs for demonstrating the relationship between various factors on particle size, PDI, Entrapment efficiency
3D graphs representing the relationship between two different factors on responses of particle size, PDI, and EE the factors with which their responses and their relationship were analyzed. Since blue color represents the lowest value; the blue area is an ideal space for estimating the role of factors for responses requiring minimum values like particle size, PDI, Entrapment efficiency whereas, red represents the high value thus, the red area is an ideal space for estimating the role of factors for responses requiring a maximum value.3D graphs give a 3D view of how each factor affects the response

Characterization of NLCs
Particle size and PDI
The optimized NLC has a particle diameter of 126 and 79 nm and PDI of 0.327 and 0.247, respectively.

Zeta Potential
The Zeta potential of the optimized formulation was -27.6mV, Zeta potential of ± 30mV is ideal. It indicates the formulation was stable and surface charge present on the particles of NLCs.
Generally, NLCs develop surface charge over a time period that leads to aggregation of particles resulting in instability. The zeta potential recorded for optimized formulation has sufficient charges to inhibit the aggregation of particles.

SEM
SEM images have shown the surface morphology of NLCs. From Photographs, Resveratrol NLC was found to be spherical. The images show the absence of free drug in the formulation at 2µ

International Journal of Pharmaceutical Research and Applications
Volume 7, Issue 1 Jan-Feb 2022, pp: 961-987 www.ijprajournal.com ISSN: 2249-7781

magnification.

Evaluation studies

Entrapment efficiency

The entrapping efficiency of NLCs was affected by the drug's solubility in solid and liquid lipids, and the concentration and ratio of the surfactants. The solid to liquid ratio also plays a prominent part in the drug's entrapment. The drug with high liquid lipid solubility has stronger Entrapment efficiency. The entrapment efficiency was found to be 70% for optimized formulation

In vitro drug release profile from NLCs

In vitro release of the drug was conducted on the optimized formulation. Sampling was done at different time periods, such as 2, 4, 6 8, 16 h, and 24 h 48, 96 hrs, and UV analysis was conducted on the samples. From the above in vitro studies, the kinetics of resveratrol released from NLCs followed zero-order kinetics.

Stability studies:

Optimized formulations were subjected to the stability study. The formulations were packed in an air tight self-sealable cover and kept in two different conditions, 25 ± 2 ^{O}C, second at 40 ± 2 ^{O}C the formulation is kept for three months, and the sample is withdrawn at the frequent intervals for analysis. Finally, the formulation was stable up to 90 days after 90 days there are only slight changes in its results.

V. CONCLUSION

In the current research, resveratrol NLC was successfully formulated through a hot homogenization technique accompanied by ultrasonication. The factors that influence formulations were determined by design expert software. Box Behnken design has been done for optimization of formulation, the optimized NLC had ideal entrapment efficiency with an average Zeta size of 126 and 79 nm. The kinetics of released resveratrol from NLCs followed zero-order and its best fit model is the Higuchi model. Finally,the release of drugs from nanoparticles was through the diffusion process. The zeta-potential is -27.6mV. It indicates that the prepared formulation was stable. Finally, the particle size was affected by the liquid lipid and solid lipid concentration. As the lipid concentration increases the size of the particle increases, The release rate and dose dumping problems can be regulated by elevating liquid and solid lipid ratio, while the entrapment efficiency rises with an elevation of solid lipid concentration. The stability of the formulations depended on the concentration of surfactants, as the ratios of water and lipid concentration change the morphology features of nanoparticles will improve. As the concentration of water is more the particles are not adhering to each other therefore stickiness between the particles was prohibited

CONFLICT OF INTEREST:

The authors declare no conflict of interest.

REFERENCES

[1]. Burns J, Yokota T, Ashihara H, Lean ME, Crozier A. Plant foods and herbal sources of resveratrol. Journal of agricultural and food chemistry. 2002 May 22;50(11):3337-40.

[2]. Agarwal A, Kharb V, Saharan VA. Process optimization, characterisation and evaluation of resveratrol-phospholipid complexes using Box-Behnken statistical design. International Current Pharmaceutical Journal. 2014 Jun 7;3(7):301-8.

[3]. Tellone E, Galtieri A, Russo A, Giardina B, Ficarra S. Resveratrol: a focus on several neurodegenerative diseases. Oxidative medicine and cellular longevity. 2015;2015.

[4]. Ghasemiyeh P, Mohammadi-Samani S. Solid lipid nanoparticles and nanostructured lipid carriers as novel drug delivery systems: applications, advantages and disadvantages. Research in pharmaceutical sciences. 2018 Aug;13(4):288.

[5]. Clare JF. Calibration of UV–vis spectrophotometers for chemical analysis. Accreditation and quality assurance. 2005 Jun 1;10(6):283-8.

[6]. Fanelli S, Zimmermann A, Totóli EG, Salgado HR. FTIR Spectrophotometry as a Green Tool for Quantitative Analysis of Drugs: Practical Application to Amoxicillin. Journal of Chemistry. 2018;2018.

[7]. Kumpugdee-Vollrath M, Ibold Y, Sriamornsak P. Solid state characterization of trans resveratrol complexes with different cyclodextrins. Journal of Asian Association of Schools of Pharmacy. 2012 Apr;1:125-36.

[8]. Saxena AK, Roy KK, Singh S, Vishnoi SP, Kumar A, Kashyap VK, Kremer L, Srivastava R, Srivastava BS. Identification and characterisation of small-molecule inhibitors of Rv3097c-encoded lipase (LipY) of Mycobacterium tuberculosis that selectively inhibit growth of bacilli in

International Journal of Pharmaceutical Research and Applications
Volume 7, Issue 1 Jan-Feb 2022, pp: 961-987 www.ijprajournal.com ISSN: 2249-7781

hypoxia. International journal of antimicrobial agents. 2013 Jul 1;42(1):27-35.

[9]. Baka E, Comer JE, Takács-Novák K. Study of equilibrium solubility measurement by saturation shake-flask method using hydrochlorothiazide as model compound. Journal of pharmaceutical and biomedical analysis. 2008 Jan 22;46(2):335-41.

[10]. Veseli A, Žakelj S, Kristl A. A review of methods for solubility determination in biopharmaceutical drug characterization. Drug development and industrial pharmacy. 2019 Nov 2;45(11):1717-24.

[11]. Sun R, Zhao G, Ni S, Xia Q. Lipid based nanocarriers with different lipid compositions for topical delivery of resveratrol: comparative analysis of characteristics and performance. Journal of Drug Delivery Science and Technology. 2014 Jan 1;24(6):591-600.

[12]. Jojo GM, Kuppusamy G, De A, Karri VN. Formulation and optimization of intranasal nanolipid carriers of pioglitazone for the repurposing in Alzheimer's disease using Box-Behnken design. Drug development and industrial pharmacy. 2019 Jul 3;45(7):1061-72.

[13]. Negi LM, Jaggi M, Talegaonkar S. Development of protocol for screening the formulation components and the assessment of common quality problems of nano-structured lipid carriers. International journal of pharmaceutics. 2014 Jan 30;461(1-2):403-10.

[14]. Vieira R, Severino P, Nalone LA, Souto SB, Silva AM, Lucarini M, Durazzo A, Santini A, Souto EB. Sucupira oil-loaded nanostructured lipid carriers (NLC): lipid screening, factorial design, release profile, and cytotoxicity. Molecules. 2020 Jan;25(3):685.

[15]. Fang CL, A Al-Suwayeh S, Fang JY. Nanostructured lipid carriers (NLCs) for drug delivery and targeting. Recent patents on nanotechnology. 2013 Jan 1;7(1):41-55.

[16]. Ferreira SC, Bruns RE, Ferreira HS, Matos GD, David JM, Brandao GC, da Silva EP, Portugal LA, Dos Reis PS, Souza AS, Dos Santos WN. Box-Behnken design: an alternative for the optimization of analytical methods. Analytica chimica acta. 2007 Aug 10;597(2):179-86.

[17]. Hasan CD. 25. SOP FOR ZETASIZER. Standard Operating Procedures for Instruments.:129.

[18]. Schroeter D, Spiess E, Paweletz N, Benke R. A procedure for rupture-free preparation of confluently grown monolayer cells for scanning electron microscopy. Journal of Electron Microscopy Technique. 1984;1(3):219-25.

[19]. Sarmento B, Ferreira DC, Jorgensen L, Van De Weert M. Probing insulin's secondary structure after entrapment into alginate/chitosan nanoparticles. European Journal of Pharmaceutics and Biopharmaceutics. 2007 Jan 1;65(1):10-7.

[20]. Navya MN, Parthiban S, Senthilkumar GP, Mani TT. Pharmaceutical and Nano Sciences.

[21]. Yadav KS, Sawant KK. Modified nanoprecipitation method for preparation of cytarabine-loaded PLGA nanoparticles. AapsPharmscitech. 2010 Sep 1;11(3):1456-65.

[22]. Makoni PA, WaKasongo K, Walker RB. Short term stability testing of efavirenz-loaded solid lipid nanoparticle (SLN) and nanostructured lipid carrier (NLC) dispersions. Pharmaceutics. 2019 Aug;11(8):397.

[23]. Sun W, Xie C, Wang H, Hu Y. Specific role of polysorbate 80 coating on the targeting of nanoparticles to the brain. Biomaterials. 2004 Jul 1;25(15):3065-71.

[24]. Patro SK, Jhansi M, Babu AS, Asief S, Babu PR. Drug-Excipient Compatability Studies using Thermal methods.

[25]. Jenning V, Thünemann AF, Gohla SH. Characterisation of a novel solid lipid nanoparticle carrier system based on binary mixtures of liquid and solid lipids. International Journal of Pharmaceutics. 2000 Apr 20;199(2):167-77.

[26]. Solanki AB, Parikh JR, Parikh RH. Formulation and optimization of piroxicam proniosomes by 3-factor, 3-level Box-Behnken design. AAPS PharmSciTech. 2007 Oct 1;8(4):43.

[27]. Neves AR, Lúcio M, Martins S, Lima JL, Reis S. Novel resveratrol nanodelivery systems based on lipid nanoparticles to enhance its oral bioavailability. International Journal of Nanomedicine. 2013;8:177.

[28]. Gandhi A, Jana S, Sen KK. In-vitro release of acyclovir loaded Eudragit RLPO®

nanoparticles for sustained drug delivery. International journal of biological macromolecules. 2014 Jun 1;67:478-82.

[29]. Reddy KA, Karpagam S. Preparation and Characterization of Drug-Loaded Phthalic Anhydride Based Hyperbranched Polyesteramide Microspheres. Pharmaceutical Chemistry Journal. 2017 Mar;50(12):857-64.